

High Pressure Polymerization of the Li-Intercalated Fulleride $\text{Li}_3\text{CsC}_{60}$

Serena Margadonna and Kosmas Prassides*

Fullerene Science Centre, School of Chemistry, Physics and Environmental Science,
University of Sussex, Brighton BN1 9QJ, United Kingdom

Kenneth D. Knudsen and Michael Hanfland

European Synchrotron Radiation Facility, B.P. 220, F-38043 Grenoble, France

Mayumi Kosaka

NEC Fundamental Research Laboratories, Tsukuba 305, Japan

Katsumi Tanigaki

Faculty of Science, Osaka City University, PREST, JST, 3-3-138 Sugimoto,
Sumiyoshi-ku, Osaka 558-8585, Japan

Received June 2, 1999. Revised Manuscript Received July 26, 1999

The structural features of the superconducting $\text{Li}_3\text{CsC}_{60}$ fulleride are studied by synchrotron X-ray powder diffraction as a function of pressure and temperature. In contrast with the behavior of $\text{Li}_2\text{CsC}_{60}$, $\text{Li}_3\text{CsC}_{60}$ shows a phase transition below room temperature from *fcc* (space group $Fm\bar{3}m$) to an orientationally ordered primitive cubic phase (space group $Pa\bar{3}$), isostructural with the metastable phases of $\text{Na}_2\text{AC}_{60}$. Despite the slow cooling protocols adopted, the system shows no other phase transitions even after prolonged standing at 200 K. The pressure dependence of the structure of $\text{Li}_3\text{CsC}_{60}$ at ambient temperature was followed up to 8.12 GPa. A phase transition occurs at 0.72 GPa to a low symmetry fullerene bridged polymeric phase with short center-to-center interfullerene separations of ~ 9.38 Å. This phase was found to be monoclinic (space group $P2_1/a$), isostructural with the low-temperature polymer phase of $\text{Na}_2\text{RbC}_{60}$ and the high-pressure polymer phase of $\text{Na}_2\text{CsC}_{60}$. The pressure evolution of the monoclinic lattice constants reveals a highly incompressible, tightly packed, and strongly anisotropic polymeric structure.

Introduction

Alkali fullerides with stoichiometry $\text{Na}_2\text{AC}_{60}$ ($A = \text{K}^+$, Rb^+ , Cs^+) display a rich structural and electronic phase diagram as a function of both pressure and temperature. At high temperatures, they adopt an orientationally disordered face-centered cubic structure ($Fm\bar{3}m$) with the Na^+ and A^+ ions residing in the tetrahedral and octahedral holes, respectively. Just below room temperature, a phase transition to an orientationally ordered primitive cubic structure ($Pa\bar{3}$) occurs. In this phase, the majority of the fulleride ions are rotated counter-clockwise by $\sim 98^\circ$ about the appropriate cube diagonal [111], with the remaining ions adopting minor orientations. The positions of the two cations do not vary significantly from the ideal octahedral and tetrahedral site, even though the lower crystal symmetry allows the displacement of Na^+ along the [111] direction.¹ Below room temperature, the structural properties of $\text{Na}_2\text{AC}_{60}$ are found to be highly sensitive to cooling protocols. While upon rapid cooling, they remain strictly cubic, slow cooling leads to a monoclinic phase comprising of quasi-one-dimensional C_{60}^{3-} chains with short interball center-to-center distances of ~ 9.38 Å and with the C_{60}^{3-} units bridged by single C–C bonds.² The kinetics of the

polymerization are extremely slow and the monomer \rightarrow polymer transformation never goes to completion.^{2,3} Structural studies of the $\text{Na}_2\text{Rb}_{1-x}\text{Cs}_x\text{C}_{60}$ ($0 \leq x \leq 1$) series⁴ have shown that polymer formation is extremely sensitive to the interfullerene separation in the precursor cubic phase with $\text{Na}_2\text{CsC}_{60}$ being completely insensitive to thermal history and remaining cubic under all cooling protocols. In this case, polymerization occurs only with the application of high pressure, which brings the interball separation below the critical value.⁵

(1) (a) Kniaz, K.; Fisher, J. E.; Zhu, Q.; Rosseinsky, M. J.; Zhou, O.; Murphy, D. W. *Solid State Commun.* **1993**, *88*, 47. (b) Christides, C.; Prassides, K.; Neumann, D. A.; Copley, J. R. D.; Mizuki, J.; Tanigaki, K.; Hirose, I.; Ebbesen, T. W. *Europhys. Lett.* **1993**, *24*, 755. (c) Prassides, K.; Christides, C.; Thomas, I. M.; Mizuki, J.; Tanigaki, K.; Hirose, I.; Ebbesen, T. W. *Science* **1994**, *263*, 950. (d) Tanigaki, K.; Hirose, I.; Manako, T.; Tsai, J. S.; Mizuki, J.; Ebbesen, T. W. *Phys. Rev. B* **1994**, *49*, 12307.

(2) (a) Prassides, K.; Vavakis, K.; Kordatos, K.; Tanigaki, K.; Benedele, G. M.; Stephens, P. W. *J. Am. Chem. Soc.* **1997**, *119*, 834. (b) Benedele, G. M.; Stephens, P. W.; Prassides, K.; Vavakis, K.; Kordatos, K.; Tanigaki, K. *Phys. Rev. Lett.* **1998**, *80*, 736. (c) Lappas, A.; Brown, C. M.; Kordatos, K.; Suard, E.; Tanigaki, K.; Prassides, K. *J. Phys. Condens. Matter.* **1999**, *11*, 371.

(3) Brown, C. M.; Takenobu, T.; Kordatos, K.; Prassides, K.; Iwasa, Y.; Tanigaki, K. *Phys. Rev. B* **1999**, *59*, 4439.

(4) Prassides, K.; Tanigaki, K.; Iwasa, Y. *Physica C* **1997**, *282*, 307.

The behavior of $\text{Li}_2\text{AC}_{60}$ ($\text{A} = \text{Rb}, \text{Cs}$) fullerides is distinctly different. Even though they have small enough lattice constants, no evidence for a symmetry-lowering structural transition is found either at ambient⁶ or at elevated pressure.⁷ Such a behavior has been rationalized in terms of the existence of strong bonding Li^+-C interactions, which preclude orientationally ordering transitions and subsequent C–C bond formation between fullerene units, despite the considerably decreased interfullerene contact distances. This interaction, not encountered in any other alkali fullerides, seems to be also responsible for the loss of superconductivity in $\text{Li}_2\text{AC}_{60}$. The formal charge of the C_{60}^{n-} ions is less than 3, implying a less than half full t_{1u} band. Raman measurements have established a value of $n \approx 2.5$.⁸ Half-filling and recovery of superconductivity ($T_c = 10.5$ K) have been successfully achieved by synthesizing the Li-overdoped salt $\text{Li}_3\text{CsC}_{60}$.⁸ High-resolution synchrotron X-ray structural work has shown that the Li^+-C interaction is now considerably weakened compared to $\text{Li}_2\text{CsC}_{60}$, and the C_{60}^{3-} ions have now the freedom to orient themselves in such a way as to minimize the electrostatic interactions. As a consequence, just below room temperature, this system shows a transition to an orientationally ordered phase, isostructural with the $P\bar{a}3$ phase of the Na-intercalated systems.⁹

In the present work we investigate the influence of the excess Li on the structural properties of $\text{Li}_3\text{CsC}_{60}$ and explore the sensitivity of its structure to slow cooling protocols and the application of pressure. Detailed synchrotron X-ray powder diffraction measurements were performed both as a function of temperature at ambient pressure and as a function of pressure at room temperature (in analogy with $\text{Na}_2\text{AC}_{60}$).^{2,5,10} No evidence of polymerization was found at ambient pressure with the primitive cubic phase also surviving to 1.07 GPa. The monomer \rightarrow polymer transformation is first encountered at 0.72 GPa with the polymer fraction growing at the expense of the cubic phase up to 1.07 GPa and then surviving to the highest pressure of the present experiments (8.12 GPa). The high-pressure polymer phase of $\text{Li}_3\text{CsC}_{60}$ has been structurally characterized to be monoclinic and isostructural with the $\text{Na}_2\text{AC}_{60}$ polymer phase.

Experimental Section

The $\text{Li}_3\text{CsC}_{60}$ sample used in the present work was prepared by reaction of stoichiometric amounts of Li and Cs with C_{60} , as described before.⁸ Phase purity was established by high-resolution synchrotron X-ray diffraction measurements.⁹ For the present work, the $\text{Li}_3\text{CsC}_{60}$ sample was sealed in a thin-wall glass capillary 0.5 mm in diameter. Synchrotron X-ray diffraction images were recorded on the Swiss-Norwegian beamline (BM1A) at the European Synchrotron Radiation

Facility (ESRF), Grenoble, with a 345-mm-diameter Mar Research circular image plate. A monochromatic X-ray beam of wavelength $\lambda = 0.8810$ Å and dimensions 0.5×0.5 mm² was focused onto the sample by sagittal bending of the second crystal of the double-crystal Si (111) monochromator. The sample was cooled from 320 to 200 K at a rate of 18 K/h. Cooling was by means of an Oxford Cryosystems Cryostream cold nitrogen blower. Images of the Debye–Sherrer rings were measured every 2 min with a sample to detector distance of 300 mm and with an exposure time of 15 s. During the data collection the sample was rotated about its axis by 30°. One-dimensional diffraction patterns were obtained by integrating around the rings using local software (program FIT2D). Data analysis was performed with the Fullprof suite of Rietveld analysis programs using the sequential refinement option.¹¹

The high-pressure X-ray diffraction experiments at ambient temperature were performed on beamline ID9 at the ESRF, Grenoble. The same $\text{Li}_3\text{CsC}_{60}$ powder sample was loaded in a diamond anvil cell (DAC), which was used for the high pressure generation and was equipped with an aluminum gasket. The diameters of the two faces of the diamond culet were 600×600 μm², and the sample was introduced in a hole made in the gasket 70 μm deep and 200 μm diameter. Silicone oil loaded in the DAC was used as a pressure medium. Pressure was increased at room temperature and was measured with the ruby fluorescence method. The diffraction patterns were collected using an image plate detector ($\lambda = 0.4995$ Å) up to a maximum pressure of 8.12 GPa. Masking of the strong Bragg reflections of the ruby crystal and integration of the two-dimensional diffraction images were performed with the local ESRF FIT2D software. Data analysis was performed with the Fullprof suite of Rietveld analysis programs.¹¹

Results

a. Structural Results at Ambient Pressure. Synchrotron X-ray powder diffraction profiles of $\text{Li}_3\text{CsC}_{60}$ were collected on slow cooling from 320 to 200 K in steps of 0.7 K at ambient pressure (Figure 1). Rietveld refinements of the diffraction data were performed at all temperatures in the 2θ range 5–29°. Above 305 K, the structure of $\text{Li}_3\text{CsC}_{60}$ is described well by the *fcc* model, in which the C_{60}^{3-} units are orientationally disordered with the Li^+ and Cs^+ ions placed in the $8c$ ($1/4, 1/4, 1/4$) and $4b$ ($1/2, 1/2, 1/2$) sites of the unit cell, respectively. The excess Li^+ ion was incorporated in the (0.375, 0.3750, 0.375) sites with an $n = 1/8$ occupancy.⁹ On further cooling, a smooth shift in the position of the cubic peaks to larger 2θ values and a change in the rate of lattice contraction are encountered, signaling the occurrence of the *fcc* to primitive cubic orientational ordering transition. The refinements show that the transition is complete just below room temperature (Figure 1 inset). Due to the low resolution of the present data, we could not distinguish between the two structures and a two-phase refinement in the coexistence region was not attempted. No evidence for additional diffraction peaks violating cubic symmetry was apparent down to 200 K (even after standing at this temperature for 6 h). This is reminiscent of the situation encountered for $\text{Na}_2\text{CsC}_{60}$ ⁵ and differs from that for $\text{Na}_2\text{-RbC}_{60}$ ² which shows the slow, incomplete phase transition to the monoclinic polymer structure in the vicinity of 250 K under the same cooling conditions.

Below 305 K, the primitive structural model with orientationally ordered C_{60}^{3-} units developed earlier for $\text{Li}_3\text{CsC}_{60}$ from high-resolution synchrotron data, was

(5) Margadonna, S.; Brown, C. M.; Lappas, A.; Prassides, K.; Tanigaki, K.; Knudsen, K. D.; Le Bihan, T.; Mezouar, M. *J. Solid State Chem.* **1999**, *145*, 471.

(6) Hirose, I.; Prassides, K.; Mizuki, J.; Tanigaki, K.; Gevaert, M.; Lappas, A.; Cockcroft, J. K. *Science* **1994**, *264*, 1294.

(7) Margadonna, S.; Brown, C. M.; Prassides, K.; Fitch, A. N.; Knudsen, K. D.; Le Bihan, T.; Mezouar, M.; Hirose, I.; Tanigaki, K. *Int. J. Inorg. Mater.* **1999**, *1*, 157.

(8) Kosaka, M.; Tanigaki, K.; Prassides, K.; Margadonna, M.; Lappas, A.; Brown, C. M.; Fitch, A. N. *Phys. Rev. B* **1999**, *59*, R6628.

(9) Margadonna, S.; Prassides, K.; Fitch, A. N.; Kosaka, M.; Tanigaki, K. *J. Am. Chem. Soc.* **1999**, *121*, 6318.

(10) Zhu, Q. *Phys. Rev. B* **1995**, *52*, 723.

(11) Rodriguez-Carvajal, Program Fullprof (version 3.5-Dec. 97), ILL (unpublished).

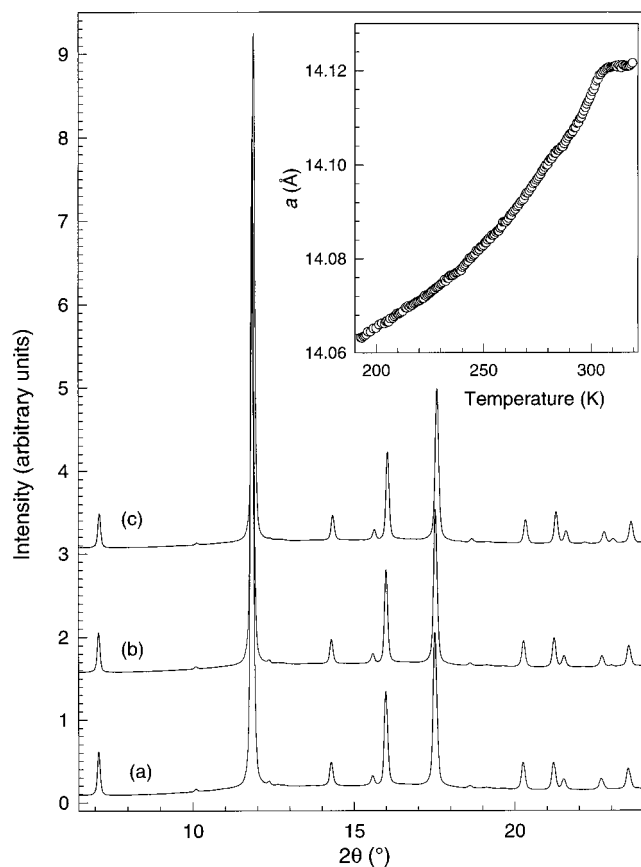


Figure 1. Synchrotron X-ray ($\lambda = 0.8810 \text{ \AA}$) powder diffraction profiles of $\text{Li}_3\text{CsC}_{60}$ at temperatures: (a) 319.5 K, (b) 290.2 K, and (c) 199.9 K. Inset: Temperature dependence of the cubic lattice constant, a , of $\text{Li}_3\text{CsC}_{60}$ obtained on cooling.

employed in the refinements.⁹ The C_{60}^{3-} ions with an average C–C bond length of 1.43 Å are rotated away from their standard orientations anticlockwise about the [111] cube diagonals by either 98° (major orientation) or 38° (minor orientation). The Li^+ and Cs^+ ions are placed in the 8c (x, x, x ; $x = 0.244$) and 4b ($1/2, 1/2, 1/2$) sites of the unit cell, respectively. The Li defect was again disordered over the corners of a cube of edge size $\sim 3.35 \text{ \AA}$ with an $1/8$ occupancy by placing it into two symmetry inequivalent positions at (x, x, x ; $x = 0.381$) and (x, y, z ; $x = y, y = z + 1/2, z = 0.381$). With the use of this structural model, the Rietveld refinements proceeded smoothly down to 200 K (cubic lattice constant at 200 K, $a = 14.0680(2) \text{ \AA}$; agreement factors, $R_{\text{wp}} = 8.2\%$, $R_{\text{exp}} = 3.7\%$). The fractional occupancy of the major orientation increased monotonically on cooling to 76.7% at 200 K, considerably larger than that found in C_{60} ,¹² implying an increased difference in energy between the two C_{60}^{3-} orientations in $\text{Li}_3\text{CsC}_{60}$. The evolution of the lattice constant, a with temperature is shown in the inset of Figure 1.

b. Structural Results at High Pressure. Synchrotron X-ray powder diffraction profiles of $\text{Li}_3\text{CsC}_{60}$ were collected at pressures between ambient and 8.12 GPa (Figure 2). Inspection of the diffraction data indicates that at ambient pressure the structure is *fcc*. As soon as a pressure of 0.39 GPa is reached, the cubic peaks

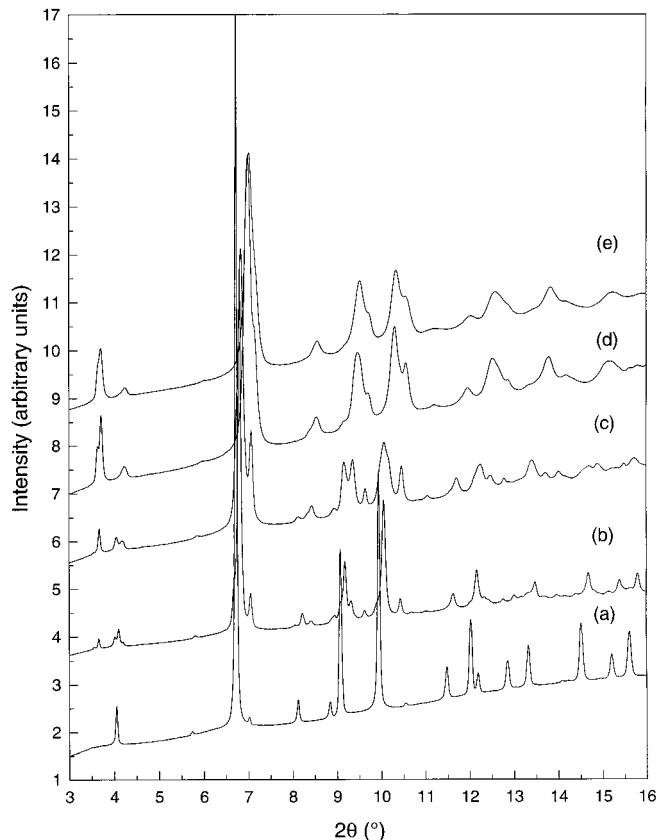


Figure 2. Synchrotron X-ray ($\lambda = 0.4995 \text{ \AA}$) powder diffraction profiles of $\text{Li}_3\text{CsC}_{60}$ at pressures: (a) 1 atm, (b) 0.72 GPa, (c) 1.45 GPa, (d) 6.26 GPa, and (e) 8.12 GPa.

shift to larger 2θ values, indicating the same primitive cubic orientational ordering transition that we encounter on cooling. At a pressure of 0.72 GPa, the diffraction pattern showed new peaks that could not be accounted for by the primitive cubic structural model. Moreover, these appear to grow with increasing pressure at the expense of the peaks assigned to the primitive cubic phase, until they completely dominate the profile at a pressure of 1.45 GPa. A detailed inspection of the profiles suggested that the new Bragg reflections could be indexed with the monoclinic space group $P2_1/a$ used before to describe the polymeric phases of $\text{Na}_2\text{AC}_{60}$.^{2,5} To extract reliable values of the lattice constants, the diffraction profiles at all pressures were analyzed by the LeBail method in the 2θ range 3.5–17°. The data collected at ambient pressure were refined with the *fcc* model ($a = 14.111(1) \text{ \AA}$; space group $Fm\bar{3}m$; agreement factors: $R_{\text{wp}} = 3.1\%$; $R_{\text{exp}} = 1.9\%$), while those at 0.38 GPa with the primitive cubic model ($a = 14.0114(3) \text{ \AA}$; space group $Pa\bar{3}$; agreement factors: $R_{\text{wp}} = 2.4\%$; $R_{\text{exp}} = 2.1\%$). The X-ray powder diffraction profiles at 0.72 and 1.08 GPa were treated using a two-phase model of coexisting monoclinic and cubic phases. The value of the cubic lattice constant was $a = 13.928(2) \text{ \AA}$, while those of the monoclinic lattice constants were $a = 13.675(2) \text{ \AA}$, $b = 14.145(1) \text{ \AA}$, $c = 9.358(1) \text{ \AA}$, and $\beta = 133.490(6)^\circ$ at 1.08 GPa, showing that a decrease in volume of 2.9-(1)% accompanies the cubic to monoclinic phase transition. For pressures in excess of 1.45 GPa, single-phase refinements with the monoclinic structural model were performed. The evolution of the monoclinic lattice parameters with pressure is shown in Figure 3.

(12) Prassides, K.; Kroto, H. W.; Taylor, R.; Walton, D. R. M.; David, W. I. F.; Tomkinson, J.; Rosseinsky, M. J.; Murphy, D. W.; Haddon, R. C. *Carbon* **1992**, *30*, 1277.

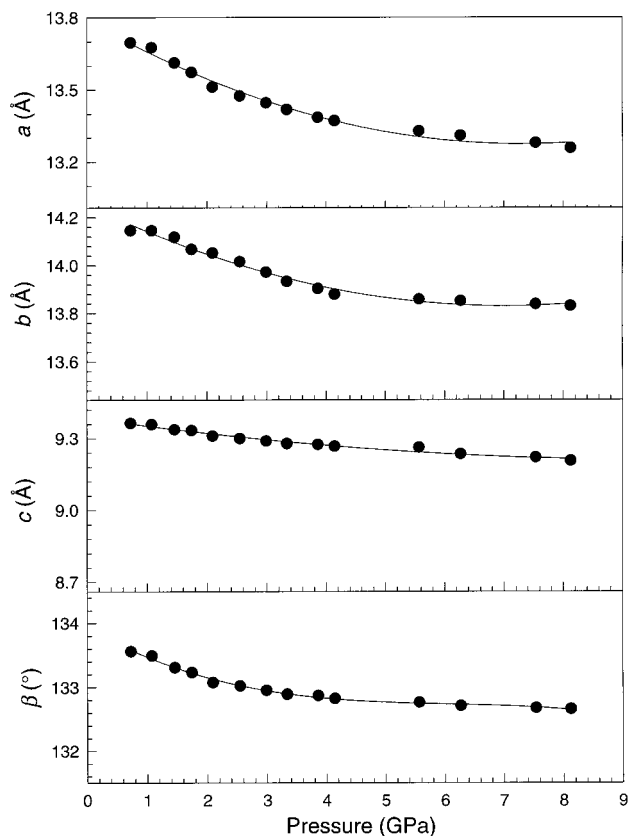


Figure 3. Pressure dependence of the lattice parameters (a , b , c , and β) of the monoclinic phase of $\text{Li}_3\text{CsC}_{60}$ at ambient temperature. The lines through the data points are guides to the eye.

The data collected at 1.45 GPa were also refined by the Rietveld method using as a starting model the quasi one-dimensional polymeric structure of $\text{Na}_2\text{CsC}_{60}$,^{2,5} in which the fullerene molecules form chains, connected via single C–C covalent bonds. Thirty symmetry-inequivalent carbon atoms are needed in space group $P2_1/a$ to generate the two C_{60}^{3-} ions, whose centers reside at the $(0, 0, 0)$ and $(\frac{1}{2}, \frac{1}{2}, 0)$ positions of the unit cell. The orientation of the C_{60}^{3-} ion at $(0, 0, 0)$ is derived from the standard orientation by an anticlockwise rotation of $\psi = 82^\circ$ about the $[001]$ direction. In this case, a single C atom is located along the monoclinic c axis, which defines the polymer chain axis. The coordinates of the C_{60}^{3-} units were kept constant during refinement, with the bridging interfullerene C–C bonds fixed at 1.55 Å. The alkali ions, Cs^+ and Li^+ , were located at the $(\frac{1}{2}, 0, 0)$ and $(x = -0.018, y = 0.266, z = 0.482)$ positions, derived from the high-symmetry octahedral and tetrahedral sites of the parent cubic structure, respectively. In the same way, we derived the position of the Li^+ defect that was also kept fixed during the refinement. The excess Li was split over four symmetry inequivalent positions, describing a cube centered at the pseudo-octahedral $(\frac{1}{2}, 0, 0)$ site with a $\frac{1}{8}$ occupancy. A stable refinement (Figure 4) was achieved with this structural model obtaining values for the monoclinic lattice constants $a = 13.62(1)$ Å, $b = 14.061(2)$ Å, $c = 9.362(2)$ Å, and $\beta = 133.48(7)^\circ$ (agreement factors: $R_{\text{wp}} = 12.1\%$, $R_{\text{exp}} = 11.7\%$). The crystal structure of the $\text{Li}_3\text{CsC}_{60}$ polymer is shown in Figure 5.

One interesting feature of the diffraction data in Figure 2 is the behavior of the low angle monoclinic

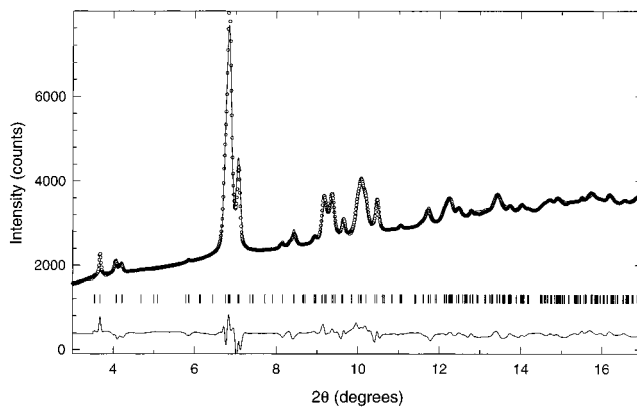


Figure 4. Final observed (open circle) and calculated (solid line) synchrotron X-ray ($\lambda = 0.4995$ Å) powder diffraction profile of $\text{Li}_3\text{CsC}_{60}$ at 1.45 GPa. The lower line shows the difference profile and the vertical marks indicate the predicted reflections.

(110) and $(11\bar{1})$ peaks with increasing pressure. As the pressure increases and the peaks shift toward high angles, there is a continuous increase in intensity. To explain this behavior, we recall that the form factor, $f(\theta)$ for hollow spherical molecules with uniform charge density ρ and radius R is given by $f(\theta) = \rho \sin(2\pi R/d) / (2\pi R/d)$, where d is the lattice spacing.^{13,14} The X-ray scattering form factor, $[f(\theta)/\rho]^2$ is then expected to show a node in the range $3.6\text{--}4.0^\circ$ for radii in the range $3.86\text{--}3.55$ Å. Thus at low pressures the low-angle peaks coincide with the zero in the form factor. As the C_{60} units are incompressible and pressure principally modulates the interfullerene separations, further increase in pressure moves them away from the minimum and their intensity grows continuously.

Discussion

The temperature-dependent synchrotron X-ray data have clearly shown the absence in $\text{Li}_3\text{CsC}_{60}$ of a phase transition to a low-symmetry phase at ambient pressure, despite the slow cooling procedures adopted. Similar cooling protocols had allowed the primitive cubic (monomer) \rightarrow monoclinic (polymer) transition to occur on cooling in the vicinity of 250 K for the closely related isostructural fullerides, $\text{Na}_2\text{KC}_{60}$ and $\text{Na}_2\text{Rb}_{1-x}\text{Cs}_x\text{C}_{60}$ ($0 \leq x < 1$),² but not for $\text{Na}_2\text{CsC}_{60}$ ⁵ and $\text{Li}_2\text{CsC}_{60}$.⁷ The origin of the differing behavior among the sodium-intercalated fullerides can be understood in terms of the existence of a critical contact distance between C_{60}^{3-} ions for C–C bonding to occur. Thus the interfullerene separation in $\text{Na}_2\text{CsC}_{60}$ ($a = 14.1073(5)$ Å at 246 K) is larger than that in $\text{Na}_2\text{RbC}_{60}$ ($a = 14.0808(8)$ Å at 248 K) by 0.2% and polymerization does not occur at ambient pressure. On the other hand, the nonoccurrence of polymerization in $\text{Li}_2\text{CsC}_{60}$ has been attributed to strong $\text{Li}^+\text{--C}$ interactions despite considerably smaller interfullerene separations than those in $\text{Na}_2\text{RbC}_{60}$. These preclude transformation to the $P2_1/a$ structure and do not allow the C_{60} molecules to orient in such a way as to encourage C–C bond formation.

(13) Duclos, S. J.; Brister, K.; Haddon, R. C.; Kortan, A. R.; Thiel, F. A. *Nature* **1991**, *351*, 380.

(14) Brown, C. M.; Beer, E.; Bellavia, C.; Cristofolini, L.; Gonzalez, R.; Hanfland, M.; Hausermann, D.; Keshavarz-K., M.; Kordatos, K.; Prassides, K.; Wudl, F. *J. Am. Chem. Soc.* **1996**, *118*, 8715.

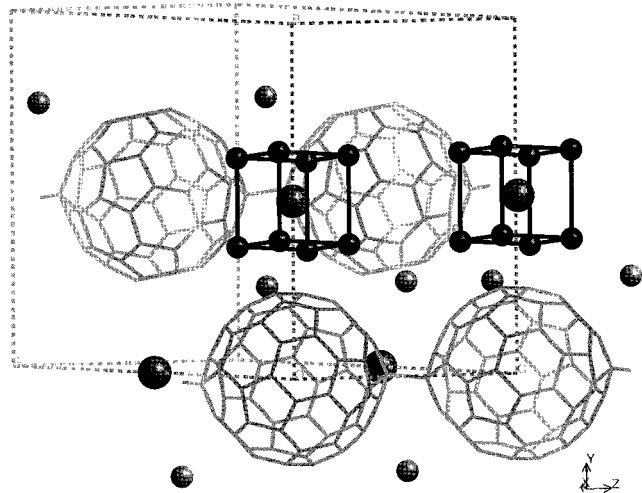


Figure 5. The crystal structure of polymerized $\text{Li}_3\text{CsC}_{60}$. The fullerenes form polymeric chains connected via single C–C bonds. The Cs^+ and Li^+ ions in the tetrahedral site are depicted as large dark and small light spheres, respectively, while the Li defect as small dark spheres. The defect around the $(\frac{1}{2}, 0, 0)$ position has been removed for clarity.

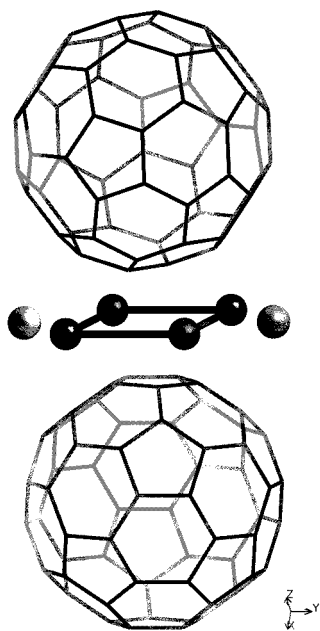


Figure 6. Schematic diagram of the arrangement of the Li ions in the primitive cubic structure of $\text{Li}_3\text{CsC}_{60}$. The defect Li ions are shaded to a darker tone than that of the tetrahedral ones.

In the present case, even though $\text{Li}_3\text{CsC}_{60}$ has a value for the interfullerene separation ($a = 14.0819(2)$ Å at 248 K) smaller than that in $\text{Na}_2\text{CsC}_{60}$ and comparable to that in $\text{Na}_2\text{RbC}_{60}$ and adopts the right precursor structure, it does not polymerize. The origin of this difference could be associated with the presence of the excess Li which lies in the interball spacing, and thus leads to an appreciable steric crowding that does not allow the C_{60} units to move close enough to form the C–C bond (Figure 6). The nonoccurrence of polymerization can be also related to the different intermolecular orientational potential that the C_{60}^{3-} ions experience due to the presence of the Li defect. The carbon bonds can form only during orientational jumps, as the fullerenes perform librational motion around their equi-

librium positions. Probably the increased steric hindrance causes a decrease in the librational amplitude and bond formation becomes less likely despite the value of the lattice constant. Such arguments are not applicable when the interfullerene separation is reduced through the application of pressure at room temperature and polymerization can then take place efficiently, as in the case of $\text{Na}_2\text{CsC}_{60}$.

The stability of the tightly packed polymer phase of $\text{Li}_3\text{CsC}_{60}$ is also affected by the steric influence of the Li^+ , Cs^+ , and defect Li ions. Each Li^+ ion that is in a pseudo-tetrahedral site ($x = -0.018$, $y = 0.266$, $z = 0.482$) coordinates to three 6:5 (fusing hexagon and pentagons) C–C and one 6:6 (fusing two hexagon) C–C bonds. At 1.45 GPa, the average $\text{Li}^+ - \text{C}_{60}^{3-}$ distance is 2.81 Å, presenting no steric crowding. On the other hand, some steric hindrance is caused by the Cs^+ ion as it coordinates to four 6:5 and two 6:6 C–C bonds with an average distance of 3.4 Å that is somewhat smaller than the sum of the ionic radius of Cs^+ and the van der Waals radius of C. However, the major steric effect arises from the excess Li which is disordered over the corners of a cubic $(\text{Li}_{1/8})_8$ cluster centered on the pseudo-octahedral positions with an edge size of 3.40 Å (cf., Li–Li distance of 3.04 Å in Li metal). Inspection of the shortest contacts between the defect and the Li^+ or Cs^+ ions do not show any unfavorable contacts, but a full examination of all $\text{Li} - \text{C}_{60}^{3-}$ distances reveals contacts of 2.2 Å for the Li defect. These are shorter than the sum of the ionic radius of Li^+ and the van der Waals radius of C creating considerable steric crowding along the a and b monoclinic axes, where the pseudo-octahedral sites are positioned. The result is a substantially anisotropic structure, with different compressibility along the three monoclinic directions. The pressure evolution of the lattice constants a , b , and c (Figure 3) reveals this diverse character of bonding interactions present, with the solid being least compressible along c , the polymer chain direction of the bridging covalent C–C bonds. On the other hand, the largest compressibility is exhibited along a , with that along b (the interchain direction) assuming an intermediate value. This behavior is in sharp contrast with what is observed for the $\text{Na}_2\text{CsC}_{60}$ polymer,⁵ which is most compressible along the b direction. The difference can be traced to the excess Li present in $\text{Li}_3\text{CsC}_{60}$ and can be understood by noting the different alignment of the cube faces formed by the Li defect with respect to each of these axes (Figure 5). While the monoclinic a axis bisects the edges of the cubes formed by the defect, the b axis is perpendicular to their faces, thus leading to a greater steric hindrance along the b direction.

The pressure evolution of the volume of both the cubic and monoclinic structural variants of $\text{Li}_3\text{CsC}_{60}$ is shown in Figure 7. The volume of the primitive cubic monomer phase varies linearly in the pressure range 0.39 to 1.08 GPa, resulting in a value for the linear volume compressibility, $\kappa \equiv d \ln V/dP = 0.026(7)$ GPa^{-1} . This is smaller than that measured for $\text{Na}_2\text{CsC}_{60}$ ($0.064(4)$ GPa^{-1}) as a result of the increased steric hindrance with a tighter crystal packing. Figure 7 also includes a least-squares fit of the ambient-temperature equation of state of the monoclinic polymer phase of $\text{Li}_3\text{CsC}_{60}$ to the semiempirical second-order Murnaghan EOS:¹⁵ P

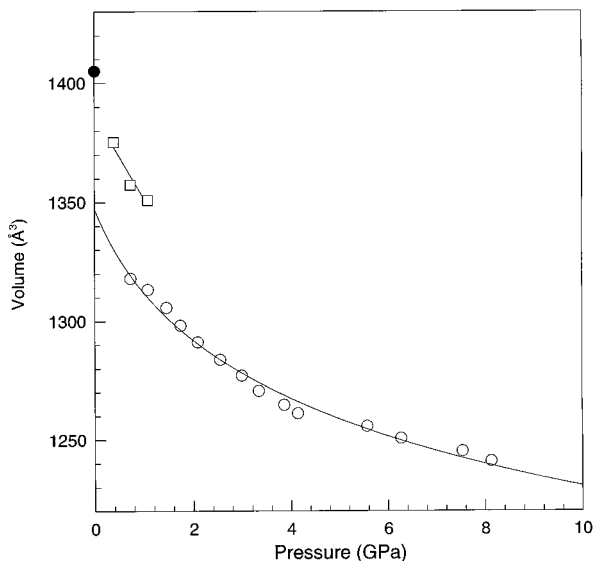


Figure 7. Pressure dependence of the volume of the *fcc* ($V/2$), primitive cubic ($V/2$) and monoclinic (V) phases of $\text{Li}_3\text{CsC}_{60}$ at ambient temperature. The full circle (●) represents the datum for the *fcc* phase; open squares, (□) the data for the primitive cubic phase; and open circles, (○) the data for the monoclinic phase. The line through the data of the monoclinic phase represents a least-squares fit to the Murnaghan equation-of-state, while that through the cubic phase is a linear fit.

$= (K_0/K_0')[(V_0/V)^{K_0'} - 1]$, where K_0 is the atmospheric pressure isothermal bulk modulus, K_0' is its pressure derivative ($= dK_0/dP$), and V_0 is the unit cell volume at zero pressure. The fit results in values of $K_0 = 26(2)$ GPa and $K_0' = 27(2)$.

(15) (a) Murnaghan, F. D. *Proc. Natl. Acad. Sci. U.S.A.* **1947**, *30*, 244. (b) Macdonald, J. R.; Powell, D. R. *J. Res. Natl. Bur. Stand.* **1971**, *A75*, 441.

Conclusions

Synchrotron X-ray powder diffraction measurements have been employed to investigate the structural properties of the superconducting fulleride $\text{Li}_3\text{CsC}_{60}$ at both ambient and elevated pressure. The behavior of $\text{Li}_3\text{CsC}_{60}$ is similar to that shown by the Na-containing $\text{Na}_2\text{AC}_{60}$ salts, while it differs markedly from the non-superconducting Li-containing family. Below room temperature, $\text{Li}_3\text{CsC}_{60}$ shows an orientationally ordering transition from *fcc* to primitive cubic. No other symmetry-lowering structural transition is found at ambient pressure on cooling even after prolonged standing at 200 K in close resemblance to the behavior of $\text{Na}_2\text{CsC}_{60}$. The lack of polymerization despite the appropriate interfullerene separation has been rationalized in terms of the somewhat increased steric crowding created by the Li defect which precludes C–C bond formation between fullerene units. The primitive cubic phase survives upon application of pressure to 1.08 GPa when a transition occurs to a monoclinic phase, which comprises of quasi-one-dimensional singly bonded C–C C_{60}^{3-} chains. The Li defect is disordered at the corners of a cube with an edge length of 3.4 Å, centered at the pseudo-octahedral position along the *a* and *b* monoclinic axes. The increased steric hindrance caused by the Li excess results in a tightly packed polymeric phase that is strongly anisotropic.

Acknowledgment. We thank NEDO FCT for financial support, the European Synchrotron Radiation Facility (ESRF) for provision of synchrotron X-ray beamtime and C. M. Brown and A. Lappas for help with the experiments. K.T. also thanks the Sumitomo Foundation for partial support.

CM990346C